

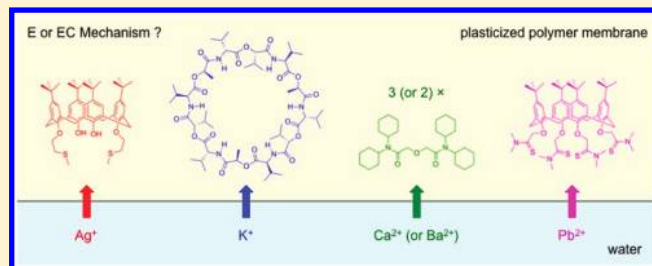
# Electrochemical Mechanism of Ion–Ionophore Recognition at Plasticized Polymer Membrane/Water Interfaces

Ryoichi Ishimatsu,<sup>†</sup> Anahita Izadyar, Benjamin Kabagambe, Yushin Kim, Jiyeon Kim, and Shigeru Amemiya\*

Department of Chemistry, University of Pittsburgh, 219 Parkman Avenue, Pittsburgh, Pennsylvania, 15260

**S** Supporting Information

**ABSTRACT:** Here, we report on the first electrochemical study that reveals the kinetics and molecular level mechanism of heterogeneous ion–ionophore recognition at plasticized polymer membrane/water interfaces. The new kinetic data provide greater understanding of this important ion-transfer (IT) process, which determines various dynamic characteristics of the current technologies that enable highly selective ion sensing and separation. The theoretical assessment of the reliable voltammetric data confirms that the dynamics of the ionophore-facilitated IT follows the one-step electrochemical (E) mechanism controlled by ion–ionophore complexation at the very interface in contrast to the thermodynamically equivalent two-step electrochemical–chemical (EC) mechanism based on the simple transfer of an aqueous ion followed by its complexation in the bulk membrane. Specifically, cyclic voltammograms of  $\text{Ag}^+$ ,  $\text{K}^+$ ,  $\text{Ca}^{2+}$ ,  $\text{Ba}^{2+}$ , and  $\text{Pb}^{2+}$  transfers facilitated by highly selective ionophores are measured and analyzed numerically using the E mechanism to obtain standard IT rate constants in the range of  $10^{-2}$  to  $10^{-3}$  cm/s at both plasticized poly(vinyl chloride) membrane/water and 1,2-dichloroethane/water interfaces. We demonstrate that these strongly facilitated IT processes are too fast to be ascribed to the EC mechanism. Moreover, the little effect of the viscosity of nonaqueous media on the IT kinetics excludes the EC mechanism, where the kinetics of simple IT is viscosity-dependent. Finally, we employ molecular level models for the E mechanism to propose three-dimensional ion–ionophore complexation at the two-dimensional interface as the unique kinetic requirement for the thermodynamically facilitated IT.



## INTRODUCTION

Current technologies for highly selective ion sensing<sup>1</sup> and separation<sup>2</sup> are chemically based on the recognition of an aqueous target ion by a membraneous ionophore, which thermodynamically facilitates selective ion transfer (IT) into a plasticized polymer membrane. During the past five decades, >1000 natural and synthetic ionophores have been tested as selective recognition elements of such potentiometric and optical sensors for various analyte ions.<sup>3</sup> Especially successful are ionophores for alkaline, alkaline earth, and heavy metal ions, for example, ionophores 1–4 (Figure 1), which can render plasticized polymer membranes up to  $10^{10}$ – $10^{15}$  times selective for a target ion against interfering ions.<sup>1c</sup> This high selectivity is ascribed to the formation of ion–ionophore complexes with unique stoichiometries,  $n$ , and large overall formation constants,  $\beta_n$ , in the bulk membrane. For instance, ionophores 1, 2, and 4 form stable 1:1 complexes with  $\text{Ag}^+$ ,  $\text{K}^+$ , and  $\text{Pb}^{2+}$ , respectively, to yield  $\beta_1$  values of  $\sim 10^{10}$ – $10^{15}$  in plasticized poly(vinyl chloride) (PVC) membranes, where a large  $\beta_3$  value of  $\sim 10^{30}$  was also determined for 1:3  $\text{Ca}^{2+}$ –ionophore 3 complexes.<sup>4</sup> The strong ion–ionophore interaction overcomes an unfavorable change in the free energy of the transfer of the hydrophilic ions into the hydrophobic membrane. Moreover, the thermodynamically facilitated IT has been assumed to be fast and instantaneously reach local equilibrium across the interface even under dynamic mass-transport

conditions, thereby developing the phase boundary potential as expected from the Nernst equation.<sup>1b</sup> The resulting potential is unfavorable for the transfer of an interfering ion with weaker ionophore-binding ability and/or higher hydrophilicity than the target ion to yield excellent thermodynamic selectivity.

The fundamental mechanism of facilitated IT is dynamic and electrochemical as demonstrated by employing voltammetry at interfaces between two immiscible electrolyte solutions (ITIES) such as water and 1,2-dichloroethane (DCE).<sup>5</sup> Kinetic analysis is essential for discrimination between two thermodynamically equivalent mechanisms of IT facilitated by lipophilic ionophores, that is, one-step electrochemical (E) mechanism and two-step electrochemical–chemical (EC) mechanism.<sup>6</sup> Specifically, the EC mechanism is based on the simple transfer of an ion across the ITIES followed by its homogeneous complexation with an ionophore in the nonaqueous phase, while the overall transfer process is considered as a single interfacial process in the E mechanism.<sup>7</sup> The EC mechanism is inconsistent with diffusion-limited voltammograms of rapid facilitated IT as typically observed at macroscopic ITIES because the electrochemically and chemically reversible ( $\text{E}_r\text{C}_r$ ) responses require that the dissociation of stable ion–ionophore complexes in the bulk

Received: August 3, 2011

Published: September 01, 2011

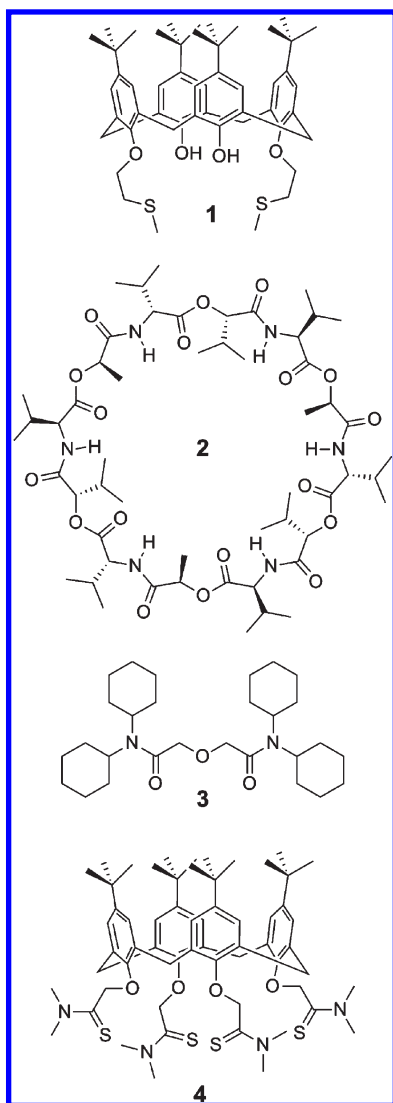


**Figure 1.** Structures of ionophores 1–4 for  $\text{Ag}^+$ ,  $\text{K}^+$ ,  $\text{Ca}^{2+}$  (and  $\text{Ba}^{2+}$ ), and  $\text{Pb}^{2+}$ , respectively.

phase must be faster than a diffusion limit.<sup>6</sup> On the other hand, the E mechanism agrees well with not only reversible voltammograms, but also kinetically limited voltammograms as obtained using microscopic<sup>8</sup> and nanoscopic<sup>9</sup> ITIES formed at the tip of glass pipets to achieve high mass transport conditions. The phenomenological Butler–Volmer-type kinetic model<sup>10</sup> was employed in the E mechanism to yield large standard IT rate constants,  $k^0$ , of  $2\text{--}10^{-2}$  cm/s and transfer coefficients,  $\alpha$ , in a normal range of 0.4–0.6.<sup>8,9</sup> Noticeably, these kinetic voltammograms have not been used to assess the EC mechanism.

Despite pioneering work by Buck and co-workers,<sup>11</sup> kinetic studies of facilitated IT at plasticized polymer membrane/water interfaces have been scarce and controversial, which seriously limits our understanding of various dynamic characteristics of the ionophore-based sensors such as response time,<sup>12</sup> detection limit,<sup>13</sup> and selectivity in mixed ion solutions<sup>14</sup> in addition to the efficiency of ion separation across ionophore-doped polymer membranes.<sup>15</sup> The major obstacle in the quantitative voltammetric measurement of IT kinetics at polymer membrane/water interfaces is a large Ohmic potential drop in the viscous, thick,

and resistive membrane even when small current at a micro-meter-sized interface is measured.<sup>16</sup> Apparently nonreversible voltammograms of  $\text{K}^+$  and  $\text{Na}^+$  transfers facilitated by ionophore 2 (valinomycin) at the microinterfaces were ascribed not to the kinetic effect but to the effect of uncompensated Ohmic potential drop on reversible IT.<sup>16b</sup> Controversially, earlier amperometric and impedance studies of the respective IT processes gave extremely small  $\alpha$  ( $\approx 0.05$ <sup>11b</sup>) and  $k^0$  ( $\approx 10^{-5}$  cm/s<sup>17</sup>) values, which indicate slow IT kinetics. Recently, we introduced a thin plasticized PVC membrane (0.7–3  $\mu\text{m}$  in thickness) supported on a solid electrode to enable quantitative IT voltammetry without a significant Ohmic potential drop.<sup>18</sup> With this new voltammetric setup, a conducting polymer film serves as the intermediate layer between the ionic PVC membrane and the electronic solid support to mediate ion-to-electron transduction, where the reduction (or oxidation) of the conducting polymer film drives the transfer of aqueous (or membraneous) cations into the opposite phase. No kinetic study, however, has been reported using such thin PVC membranes, which have been successfully applied for voltammetric/amperometric ion sensing with conducting polymers<sup>18,19</sup> or redox molecules<sup>20</sup> as ion-to-electron transducers.

Here, we report on the first electrochemical study that reveals the kinetics and molecular level mechanism of facilitated IT at plasticized PVC membrane/water interfaces to augment our understanding of this important charge transfer process for better ion sensing and separation. Specifically, we apply IT cyclic voltammetry (CV) at solid-supported thin PVC membranes<sup>18</sup> to confirm the E mechanism with  $k^0$  values of  $10^{-2}\text{--}10^{-3}$  cm/s and normal  $\alpha$  values of 0.45–0.50 for  $\text{Ag}^+$ ,  $\text{K}^+$ ,  $\text{Ca}^{2+}$ ,  $\text{Ba}^{2+}$ , and  $\text{Pb}^{2+}$  transfers facilitated by ionophores 1–4 using 2-nitrophenyl octyl ether ( $\text{oNPOE}$ ) as a common plasticizer for practical ion sensing<sup>1</sup> and separation.<sup>2</sup> We demonstrate that these IT processes are relatively slow as E processes but are too fast to be explained by the EC mechanism, where not only ion–ionophore complexation must be faster than a diffusion limited rate,<sup>6</sup> but also simple IT must be much faster than the fastest simple IT reported so far. Interestingly, we also find that these facilitated IT processes with the highly viscous  $\text{oNPOE}/\text{PVC}$  membrane can be as fast as or even faster than those with the fluidic DCE phase. This finding also excludes the EC mechanism, where simple IT is slower with a more viscous solvent medium.<sup>21</sup> Finally, the E mechanism is assessed microscopically to propose the kinetic importance of three-dimensional ion–ionophore complexation at the two-dimensional interface.

## EXPERIMENTAL SECTION

**Chemicals.** Ionophores 1–4 (Figure 1), tetradodecylammonium (TDDA) bromide, tetrapropylammonium chloride, PVC (high molecular weight), and  $\text{oNPOE}$  were obtained from Aldrich (Milwaukee, WI). Potassium tetrakis(pentafluorophenyl)borate (TFAB) was from Boulder Scientific Company (Mead, CO). All reagents were used as received. The TFAB salt of TDDA was prepared by metathesis.<sup>18a</sup> 2-*n*-Tetradecyl-2,3-dihydro-thieno[3,4-*b*][1,4]dioxine (EDOT- $\text{C}_{14}$ ) was synthesized as reported elsewhere.<sup>22</sup> Aqueous sample solutions were prepared with 18.3 M $\Omega$  cm deionized water (Nanopure, Barnstead, Dubuque, IA).

**Electrode Modification.** A 5 mm-diameter Au or glassy carbon (GC) disk attached to a rotating disk electrode tip (Pine Research Instrumentation, Raleigh, NC) was cleaned as follows to be modified with a conducting polymer film and then with an  $\text{oNPOE}$ -plasticized

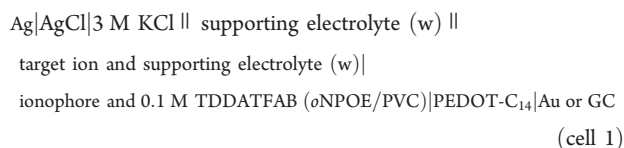
PVC membrane. A Au or GC electrode was polished with alumina paste slurry (0.3 and 0.05  $\mu\text{m}$ ) on microcloth pads (Buehler, Lake Bluff, IL). A polished Au electrode was sonicated in  $\text{H}_2\text{SO}_4$  containing 3%  $\text{K}_2\text{Cr}_2\text{O}_7$  for 15 min and in deionized water three times for 15 min. A polished GC electrode was cleaned using a UV/ozone cleaner (UV-tip Cleaner, BioForce Nanosciences, Ames, IA) for 3 min and sonicated twice in methanol and twice in water (each for 15 min).

EDOT- $\text{C}_{14}$  was electropolymerized by cyclic voltammetry to coat a clean Au or GC electrode with the polymer film (PEDOT- $\text{C}_{14}$ ). A three-electrode cell was set up with a  $\text{Ag}/\text{Ag}^+$  reference electrode (CH Instruments) and a Pt-wire counter electrode in the acetonitrile solution of 0.03 M TDDATFAB and 0.1 M EDOT- $\text{C}_{14}$ . The film deposition was conducted by cycling the potential of a GC electrode 4 times between  $-0.50$  and  $1.39$  V at  $0.1$  V/s (or twice between  $-0.70$  and  $1.5$  V for a Au electrode) using a computer-controlled CHI 600A electrochemical workstation (CH Instruments). The modified electrode was soaked in acetonitrile for 1 min to remove the residual monomer solution and soluble fractions of the film. The potential of the modified electrode in the monomer-free acetonitrile solution of 0.03 M TDDATFAB was cycled twice between  $-0.7$  and  $0.8$  V at  $0.1$  V/s, and then linearly swept to  $0.8$  V to oxidatively dope the PEDOT- $\text{C}_{14}$  film with TFAB.

Finally, a PEDOT- $\text{C}_{14}$ -modified Au or GC electrode was drop-cast with an  $\text{oNPOE}$ -plasticized PVC membrane from the  $18$   $\mu\text{L}$  THF solution prepared by dissolving  $4.0$  mg of PVC,  $16.0$  mg of  $\text{oNPOE}$ , and  $2.2$  mg of TDDATFAB in  $1$  mL THF. The THF solution also contained an ionophore to give its membrane concentration as specified in legends of the corresponding figures after THF was slowly evaporated from the drop-cast solution at least for 20 min.

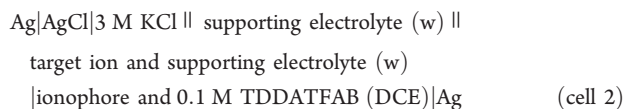
**IT Cyclic Voltammetry.** CVs of facilitated IT at plasticized PVC membrane/water and DCE/water interfaces were measured using a CHI 660B electrochemical workstation equipped with CHI 200 picoampere booster and Faraday cage (CH Instruments). All electrochemical experiments were performed at  $22 \pm 3$   $^\circ\text{C}$ . Concentrations of target ion, ionophore, and supporting electrolyte in the following electrochemical cells are given in legends of the corresponding figures. The current carried by cation transfer from the aqueous phase to the nonaqueous phase is defined to be positive.

CV with PVC/PEDOT- $\text{C}_{14}$ -modified electrodes employed a three-electrode arrangement with a double-junction  $\text{Ag}/\text{AgCl}$  reference electrode (BASi, West Lafayette, IN) and a Pt-wire counter electrode. Electrochemical cells were as follows:



A piece of Teflon tube was put on a membrane-modified electrode to obtain a disk-shaped PVC membrane/water interface with the diameter of  $1.5$  mm and the interfacial area of  $0.0177$   $\text{cm}^2$ .<sup>18</sup>

Micropipet CV employed two-electrode cells as represented by



For  $\text{Pb}^{2+}$ , a  $\text{Ag}/\text{AgCl}$  wire was used as an aqueous electrode instead. A  $4$ – $5$   $\mu\text{m}$ -diameter glass micropipet was prepared using a laser-based pipet puller (model P-2000, Sutter Instrument), modified with trimethylchlorosilane, and filled with a DCE solution as reported elsewhere.<sup>23</sup> A dual beam instrument (SMI3050SE FIB-SEM, Seiko Instruments, Chiba, Japan) was employed to mill the tapered end of a pulled micropipet by the focused beam of high-energetic gallium ions,<sup>24</sup> thereby yielding a smoother tip for better support of the microinterface.

## RESULTS AND DISCUSSION

**Kinetic Effect on Facilitated IT at Plasticized PVC Membrane/Water Interfaces.** Here, we demonstrate unambiguous and quantitative kinetic effect on facilitated IT at plasticized polymer membrane/water interfaces, which resolves long-standing controversy on the intrinsic rate of this practically important and fundamentally unique charge transfer process.<sup>1b,11,16b</sup> The kinetic effect was observed by cyclic voltammetry at Au or GC electrodes modified with a PEDOT- $\text{C}_{14}$  membrane and then with an  $\text{oNPOE}$ -plasticized PVC membrane (cell 1). The thickness of each membrane was optimized for kinetic measurement. An Ohmic potential drop was negligible in an  $\text{oNPOE}/\text{PVC}$  membrane with an estimated thickness of  $14$   $\mu\text{m}$ ,<sup>18a</sup> which was chosen in this work to achieve the semi-infinite diffusion of ion–ionophore complexes in the solid-supported membrane. A PEDOT- $\text{C}_{14}$  film with a thickness of  $0.3$ – $0.6$   $\mu\text{m}$  as estimated by SEM was used as an ion-to-electron transducer with sufficient redox capacity to avoid the significant polarization of the PVC/PEDOT- $\text{C}_{14}$ /electrode junction. These voltammetric features that are essential for reliable kinetic measurement were confirmed by reversible CVs of simple tetrapropylammonium transfer (Figure S-1).

The kinetic effect is clearly seen as wide separations of peak potentials in CVs of monovalent cations ( $\text{Ag}^+$  and  $\text{K}^+$ ) and divalent cations ( $\text{Ba}^{2+}$ ,  $\text{Ca}^{2+}$ , and  $\text{Pb}^{2+}$ ) at PVC membranes doped with ionophores 1–4 (Figure 2). In these CVs, potentials are defined against the formal potential of facilitated IT,  $E^0$ , as determined below. Facilitated  $\text{Ag}^+$  and  $\text{K}^+$  transfers (Figure 2, panels a and b, respectively) are nearly reversible at a potential sweep rate,  $\nu$ , of  $50$  mV/s to give a peak separation of  $\sim 63$  mV, which is close to  $60/z$  mV as expected for the reversible transfer of a monovalent ion with a charge of  $z = 1$ .<sup>25</sup> At a higher sweep rate, forward and reverse peak potentials shift toward more extreme potentials. A wider peak separation of  $\sim 110$  mV at  $\nu = 1$  V/s clearly indicates quasi-reversible IT. Similarly, a peak separation for relatively fast  $\text{Ba}^{2+}$  transfer (the right CVs in Figure 2c) increases from a reversible limit of  $\sim 30$  mV for  $z = 2$  to a quasi-reversible value of  $55$  mV as  $\nu$  varies from  $50$  mV/s to  $1$  V/s. On the other hand, facilitated  $\text{Ca}^{2+}$  and  $\text{Pb}^{2+}$  transfers (Figure 2, panels c and d, respectively) are slow enough to be kinetically limited even at  $\nu = 50$  mV/s as confirmed by the corresponding peak separations of  $47$  and  $100$  mV, respectively. The peak separations vary with  $\nu$ , thereby confirming kinetic control.

Noticeably, both kinetic and thermodynamic effects are clearly seen in CVs of  $\text{Ca}^{2+}$  and  $\text{Ba}^{2+}$  transfers facilitated by ionophore 3 (Figure 2c). Forward and reverse waves of the  $\text{Ca}^{2+}$  transfer are broader and more widely separated from each other than those of the  $\text{Ba}^{2+}$  transfer, indicating that the former process is slower than the latter process. In addition, the transfer of more hydrophilic  $\text{Ca}^{2+}$  is observed at more positive potentials than the  $\text{Ba}^{2+}$  transfer, which gives  $E^0 = -0.140$  V against the  $E^0$  value for  $\text{Ca}^{2+}$  as used in Figure 2c. This result indicates that ionophore 3 forms more stable complexes with  $\text{Ca}^{2+}$  than with  $\text{Ba}^{2+}$  to thermodynamically facilitate the  $\text{Ca}^{2+}$  transfer more effectively.

**Electrochemical Mechanism at Plasticized PVC Membrane/Water Interfaces.** Kinetically controlled CVs of facilitated IT at interfaces between water and the  $\text{oNPOE}$ -plasticized PVC membrane fit well with theoretical CVs (Figure 2) to validate the E mechanism, which is formulated as follows. In this

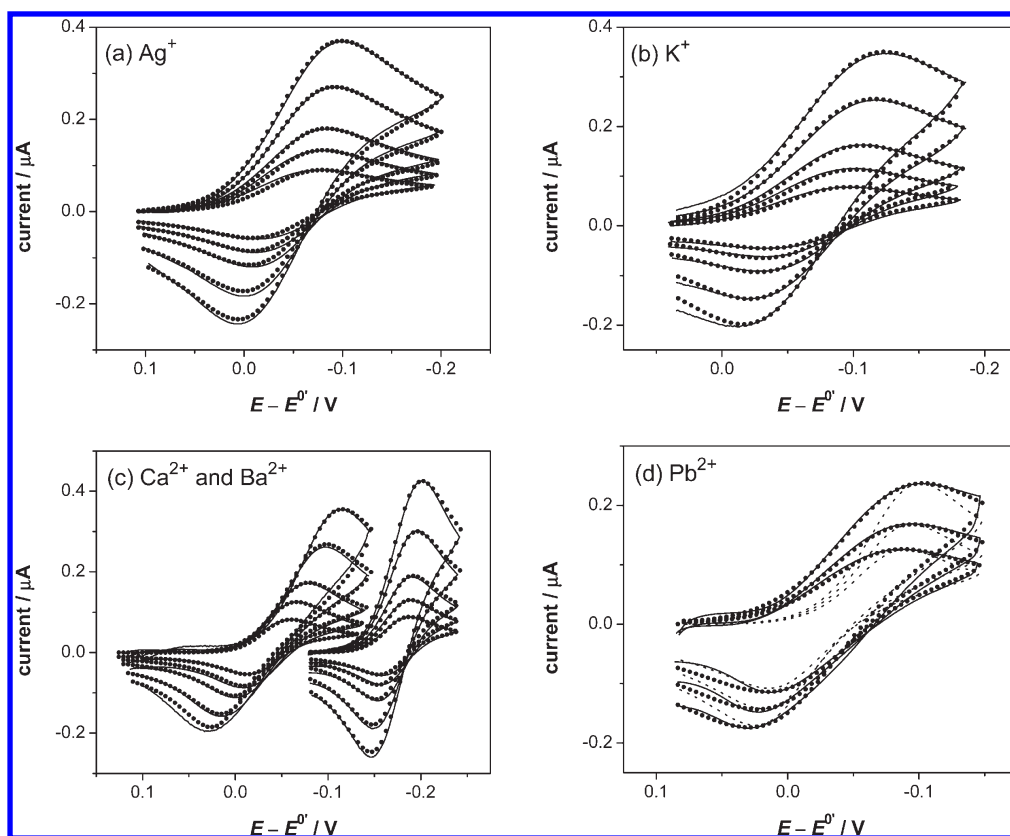


**Figure 2.** Background-subtracted CVs (solid lines) of facilitated IT as obtained using PVC/PEDOT- $C_{14}$ -modified (a and d) Au or (b and c) GC electrodes in cell 1 containing (a) 20 mM ionophore 1 with 20  $\mu\text{M}$   $\text{CH}_3\text{COOAg}$  in 10 mM  $\text{CH}_3\text{COOLi}$  (pH 5.4), (b) 20 mM ionophore 2 with 20  $\mu\text{M}$  KCl in 10 mM  $\text{Li}_2\text{SO}_4$ , (c) 60 mM ionophore 3 with 10  $\mu\text{M}$   $\text{CaCl}_2$  (left) or  $\text{BaCl}_2$  (right) in 10 mM  $\text{CH}_3\text{COOK}$  (pH 7.1), and (d) 20 mM ionophore 4 with 20  $\mu\text{M}$   $\text{PbCl}_2$  in 5 mM  $\text{MgCl}_2$  (pH 4.7). The  $E^{\circ'}$  value for  $\text{Ca}^{2+}$  is used in (c). Potential sweep rates are from the top to the bottom (a–c) 1, 0.5, 0.2, 0.1, and 0.05 V/s, and (d) 0.2, 0.1, and 0.05 V/s. Parameters for theoretical CVs (closed circles) based on the E mechanism are listed in Table 1. The dotted lines in (d) were obtained using  $z = 2$  and  $\alpha = 0.5$ .

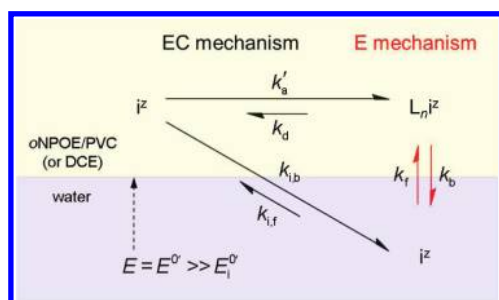
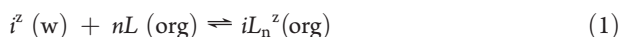


**Figure 3.** Scheme of E and EC mechanisms for facilitated IT. The rate constants are assigned to each process by eqs 2, S-2, S-6, and S-7, where  $k'_a = k_a L_n^z$ . Facilitated cation transfers are driven around  $E = E^{\circ'} \gg E_1^{\circ}$  (see eq 5).

mechanism, facilitated IT is considered as a heterogeneous one-step process, that is,



where  $i^z$  is an ion with a charge of  $z$ ,  $L$  is an electrically neutral ionophore, and  $iL_n^z$  is a 1: $n$  ion–ionophore complex. In the presence of the excess amount of ionophore, facilitated IT based on the E mechanism can be defined as a first-order

**Table 1.** Kinetic Parameters for the E Mechanism at PVC Membrane/Water Interfaces

ion/ionophore	$k^0/\text{cm s}^{-1}$	$\alpha$	$D_w/\text{cm}^2 \text{s}^{-1}$	$D_c/\text{cm}^2 \text{s}^{-1}$
$\text{Ag}^+/1$	$6.2 \times 10^{-3}$	0.45	$1.5 \times 10^{-5}$	$4.8 \times 10^{-8}$
$\text{K}^+/2$	$9.0 \times 10^{-3}$	0.48	$1.9 \times 10^{-5}$	$1.0 \times 10^{-7}$
$\text{Ba}^{2+}/3$	$1.0 \times 10^{-2}$	0.50	$1.1 \times 10^{-5}$	$7.1 \times 10^{-8}$
$\text{Ca}^{2+}/3$	$3.8 \times 10^{-3}$	0.47	$1.5 \times 10^{-5}$	$5.8 \times 10^{-8}$
$\text{Pb}^{2+}/4$	$9.7 \times 10^{-4}$	0.50 <sup>a</sup>	$9.1 \times 10^{-6}$	$2.7 \times 10^{-8}$

<sup>a</sup>  $z = 1.1$ .

process (Figure 3)

$$i^z(\text{w}) \xrightleftharpoons[k_b]{k_f} iL_n^z(\text{org}) \quad (2)$$

where  $k_f$  and  $k_b$  are first-order heterogeneous rate constants for forward and reverse transfers, respectively. The rate constants are given by Butler–Volmer-type relations as<sup>10,26</sup>

$$k_f = k^0 \exp[-\alpha z F(E - E^{\circ'})/RT] \quad (3)$$

$$k_b = k^0 \exp[(1 - \alpha)z F(E - E^{\circ'})/RT] \quad (4)$$

where  $E$  is the potential applied to the solid electrode against the reference electrode, and the formal potential,  $E^{\circ'}$ , was

chosen so that  $k_f = k_b$  at  $E = E^0$ . Consequently,  $k^0$  is independent of the membrane concentration of the excess ionophore,  $L_T$ , and the effect of the ionophore concentration on  $k_f$  and  $k_b$  as expected from the bimolecular (or multimolecular) nature of facilitated IT (eq 1) is seen in  $E^0$  as given by

$$E^0 = E_i^0 + \frac{RT}{zF} \ln \beta_n L_T^n \quad (5)$$

where  $E_i^0$  is the formal potential of simple IT. Equations 3–5 indicate that  $E^0$  represents the thermodynamic effect of  $\beta_n$  from ion–ionophore complexation in the bulk membrane, while the kinetics of ion–ionophore complexation at the interface (not in the bulk phase) determines  $k^0$  and  $\alpha$ .

The theoretical CVs based on the E mechanism with the Butler–Volmer-type first-order kinetics (eqs 3 and 4) were numerically obtained as reported elsewhere for simple IT<sup>18b</sup> to uniquely determine  $k^0$ ,  $\alpha$ ,  $E^0$ , and the diffusion coefficient of an aqueous ion,  $D_w$ , from kinetically controlled CVs (Table 1). Noticeably, negative shifts of these CVs with respect to  $E^0$  (Figure 2) result from small diffusion coefficients of ion–ionophore complexes in the viscous membrane,  $D_c$ , as quantified in recent chronoamperometric and chronopotentiometric studies.<sup>27</sup> Here, we employed CV at PVC membranes doped with the complexes to determine  $D_c$  values (Table 1), which are required for the numerical simulation (see the Supporting Information).

The numerical analysis of CVs in Figure 2 gives normal  $\alpha$  values of  $\sim 0.5$  (Table 1) to confirm the one-step E mechanism based on the Butler–Volmer-type kinetics.<sup>10</sup> Remarkably, an  $\alpha$  value of 0.48 thus determined voltammetrically for the  $K^+$  transfer facilitated by ionophore 2 contrasts to an extremely small value of  $\sim 0.05$  as obtained by amperometry of the same reaction at thick PVC membranes.<sup>11b</sup> This result supports higher reliability of our kinetic measurement with the thin PVC membrane that is free from a significant Ohmic potential drop. Moreover,  $\alpha$  values of  $\sim 0.5$  confirm the simultaneous one-step transfer of multiple charges ( $z = 2$ ) by  $Ca^{2+}$  and  $Ba^{2+}$  as the unique feature of IT<sup>8a,23,28</sup> in contrast to the stepwise transfer of multiple electrons at metal electrodes. On the other hand, CVs of facilitated  $Pb^{2+}$  transfer are broader than expected with  $z = 2$  and  $\alpha = 0.5$  (dotted lines in Figure 2d) to fit better with theoretical CVs with  $z = 1.1$  and  $\alpha = 0.5$  (closed circles). The small charge is the effective value that represents the weak potential dependence of rates for facilitated  $Pb^{2+}$  transfer, which is ascribed to a double layer effect.<sup>8a,23,28</sup> The small effective charge is not due to the transfer of  $Pb^{2+}$ –anion complexes between bulk PVC and aqueous phases. The amplitude of the observed current response is consistent with  $z = 2$ , which confirms that  $Pb^{2+}$  was transferred between the two phases. In fact,  $Cl^-$  was used as an aqueous supporting electrolyte to avoid significant ion pairing of  $Pb^{2+}$  in the aqueous phase,<sup>29</sup> although ion pairing at or near the interface may be possible to screen the charge of  $Pb^{2+}$ , thereby causing the double layer effect.

The  $k^0$  values thus determined for various combinations of ions and ionophores are similar to each other within a narrow range of  $1 \times 10^{-2}$  to  $3.8 \times 10^{-3}$  cm/s (Table 1). The fastest  $Ba^{2+}$  transfer is only  $\sim 3$  times faster than the slowest  $Ca^{2+}$  transfer, which is consistent with wider peak separations in CVs of the latter process (Figure 2c). The  $k^0$  values are lower than those reported so far for facilitated IT at ITIES ( $2\text{--}10^{-2}$  cm/s<sup>8,9</sup>), although similarly low  $k^0$  values were obtained for ionophores

**Table 2. Thermodynamic and Kinetic Parameters for the EC Mechanism at PVC Membrane/Water Interfaces**

ion/ionophore	$\beta_n$ (n)	$E^0 - E_i^0/V^a$	$k_i^0/\text{cm s}^{-1}$	$\alpha_i$	$k_a/M^{-1} \text{s}^{-1}$
$Ag^+/1$	$1.0 \times 10^{10}$ (1) <sup>b</sup>	0.49	$6.0 \times 10^1$	0.45	$>6.8 \times 10^{17}$
$K^+/2$	$4.3 \times 10^{11}$ (1) <sup>c</sup>	0.59	$5.4 \times 10^2$	0.48	$>1.7 \times 10^{18}$
$Ca^{2+}/3$	$1.6 \times 10^{29}$ (3) <sup>c</sup>	0.83	$2.4 \times 10^9$	0.47	$(>1.9 \times 10^{40d})$

<sup>a</sup> Calculated using eq 5. <sup>b</sup> From ref 4b. <sup>c</sup> From ref 4a. <sup>d</sup> With  $M^{-3} \text{s}^{-3}$ .

1–4 at DCE/water interfaces (see below). On the other hand, our  $k^0$  values are much larger than an exceptionally small value of  $\sim 10^{-5}$  cm/s as obtained by the impedance measurement of the  $Na^+$  transfer facilitated by ionophore 2, which is affected by the high bulk resistance of thick PVC membranes.<sup>17</sup>

**Assessment of the Electrochemical–Chemical Mechanism.** In comparison to the E mechanism, the EC mechanism is kinetically unfavorable when ion–ionophore complexes are stable. In the EC mechanism, facilitated IT is divided into two steps, that is, heterogeneous simple IT and homogeneous ion–ionophore complexation (eqs S-2 and S-6, respectively; see also Figure 3). Senda and co-workers excluded the EC mechanism for reversible facilitated IT at the ITIES, which requires that the dissociation of stable ion–ionophore complexes in the nonaqueous phase must be faster than a diffusion limit.<sup>6</sup> Here, we confirm the additional requirement of extremely fast simple IT for the apparently  $E_rC_r$  or  $E_qC_r$  behavior of facilitated IT, which is anticipated from the theory for EC schemes at solid electrodes.<sup>30</sup> These requirements are quantitatively evaluated by employing the EC mechanism for the numerical analysis of quasi-reversible CVs of  $Ag^+$ ,  $K^+$ , and  $Ca^{2+}$  transfers (Figure S-4; see Supporting Information), where  $\beta_n$  values are known to uniquely determine the standard rate constant for simple IT,  $k_i^0$ , and the rate constant for ion–ionophore association,  $k_a$ , in addition to the transfer coefficient,  $\alpha_i$  (Table 2).

The EC mechanism is kinetically unfavorable when strong cation–ionophore complexation causes the voltammetric wave to shift toward  $E^0$ , which is much more positive than  $E_i^0$  (see eq 5). At  $E = E^0 \gg E_i^0$  (Figure 3), simple cation transfer from the aqueous phase into the membrane phase is dramatically slowed down as represented by kinetically unfavorable, positive overvoltages,  $\eta$ , of 0.5–0.8 V, which were estimated as differences between  $E^0$  and  $E_i^0$  using eq 5 with  $\beta_n$  values reported for  $Ag^+$ ,  $K^+$ , and  $Ca^{2+}$  complexes of ionophores 1–3, respectively (Table 2). With these  $\eta$  values, rate constants for the simple transfer of aqueous cations into the membrane,  $k_{i,b}$  are  $10^5\text{--}10^9$  times lower than the corresponding  $k_i^0$  value with a normal  $\alpha_i$  value of 0.5 (eq S-3). Subsequently, extremely large  $k_i^0$  values of  $6.0 \times 10^1$  to  $2.4 \times 10^9$  cm/s (Table 2) must be employed for theoretical CVs based on the EC mechanism to fit with quasi-reversible CVs of  $Ag^+$ ,  $K^+$ , and  $Ca^{2+}$  transfers (Figure S-4; note that potentials are against  $E_i^0$ ). These  $k_i^0$  values are several orders of magnitude larger than the largest value reported so far for simple IT at PVC membrane/water interfaces, that is, 0.01 cm/s for tetraethylammonium.<sup>31</sup>

In addition, the numerical analysis based on the EC mechanism (Figure S-4) require that rate constants for ion–ionophore association,  $k_a$ , for  $Ag^+$  and  $K^+$  complexes by far exceed a diffusion-limited value of  $k_{a,d} = 1 \times 10^9 \text{ M}^{-1} \text{ s}^{-1}$  for 1:1 complexation in the bulk PVC

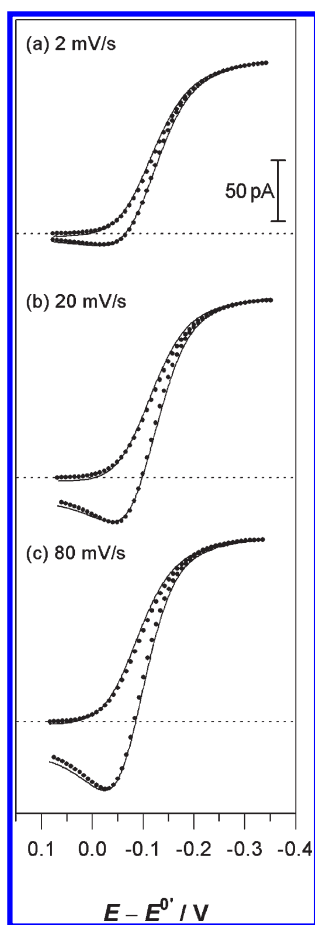


**Figure 4.** Background-subtracted micropipet CVs (solid lines) of facilitated  $\text{Ag}^+$  transfer at DCE/water microinterfaces with 20 mM ionophore 1 in cell 2 containing 100  $\mu\text{M}$   $\text{CH}_3\text{COOAg}$  in 10 mM  $\text{CH}_3\text{COOLi}$  (pH 5.5). Parameters for the theoretical CVs (closed circles) based on the E mechanism are listed in Table 3. Pipet inner diameter, 4.3  $\mu\text{m}$ .

membrane as estimated by<sup>32</sup>

$$k_{a,d} = 4\pi N_A(D_L + D_i)d \quad (6)$$

where  $N_A$  is the Avogadro's number,  $d$  ( $= 1.5 \times 10^{-7}$  cm) is the ionophore–ion separation at their collision, and  $D_L$  and  $D_i$  ( $= 5 \times 10^{-7}$   $\text{cm}^2/\text{s}$ ) are diffusion coefficients of free ionophore and free ion in the membrane. For a given  $\beta_n$  value, the rapid formation of ion–ionophore complexes corresponds to their rapid dissociation (eq S-7), which is required for yielding a current response on the reverse potential sweep (Figure 2) while strong ion–ionophore association drives the overall IT toward a chemically irreversible limit (Figure 3).

Also, we carried out numerical simulations using different  $\beta_n$  values to demonstrate that the EC mechanism can be important only when ion–ionophore complexation is weak. For instance, quasi-reversible CVs of facilitated  $\text{Ag}^+$  transfer (Figure 2a) were fitted very well with the CVs simulated using  $\beta_1$  values of  $10^{10} - 10^2$  (data not shown), thereby yielding kinetic parameters as listed in Table S-1. When  $\beta_1 < 10^4$ ,  $k_a$  values are lower than the diffusion-limited value (eq 6), and relatively small  $k_i^0$  values of  $< 0.1$  cm/s are required for the quasi-reversible responses. Therefore,  $k_a$  (or  $k_4$ ) and  $k_i^0$  must be known to assess the validity of the

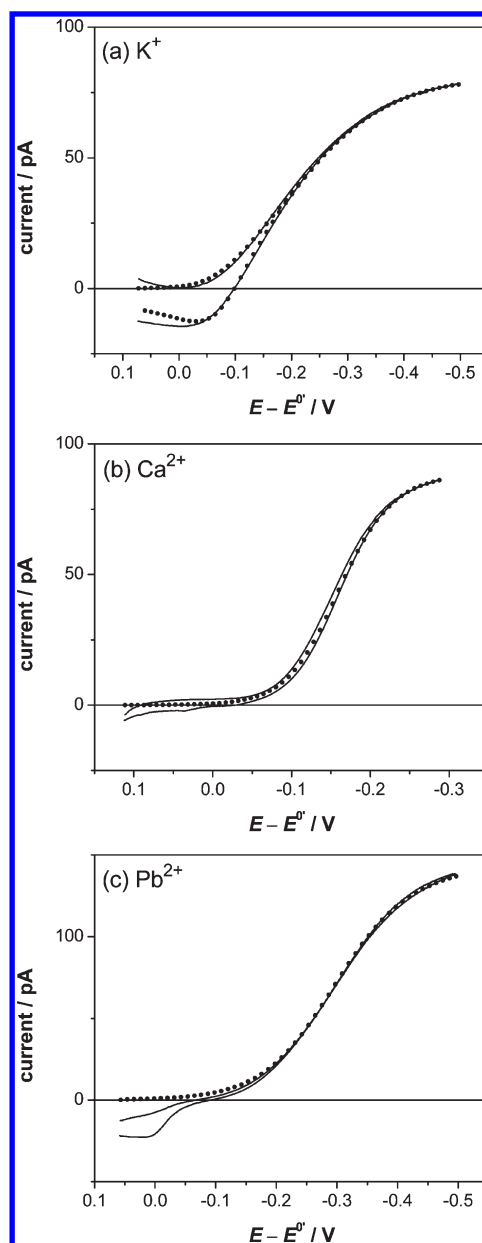


**Figure 5.** Background-subtracted micropipet CVs (solid lines) at DCE/water microinterfaces in cell 2 containing (a) 20 mM ionophore 2 with 25  $\mu\text{M}$   $\text{K}_2\text{SO}_4$  in 10 mM  $\text{MgSO}_4$  (pH 6.6), (b) 60 mM ionophore 3 with 30  $\mu\text{M}$   $(\text{CH}_3\text{COO})_2\text{Ca}$  in 10 mM  $\text{CH}_3\text{COOK}$  (pH 7.3), and (c) 20 mM ionophore 4 with 90  $\mu\text{M}$   $\text{PbCl}_2$  in 5 mM  $\text{MgCl}_2$  (pH 4.7). Parameters for theoretical CVs (closed circles) based on the E mechanism are listed in Table 3. Pipet inner diameters, (a) 3.7, (b) 4.2, and (c) 3.7  $\mu\text{m}$ . Potential sweep rates, (a) 20, (b) 5, and (c) 20 mV/s.

EC mechanism in the limit of very weak ion–ionophore complexation. The formation of a weak complex is relevant to the facilitated transfer of an interfering ion. In contrast, the EC mechanism is unambiguously excluded for the systems investigated in this work, where ionophores bind to target analytes very strongly.

Noticeably, stable 1:3<sup>4a</sup> and 1:2<sup>33</sup> ion–ionophore 3 complexes for  $\text{Ca}^{2+}$  and  $\text{Ba}^{2+}$ , respectively, must be formed at the interface to follow the E mechanism, thereby excluding the EC mechanism. In this case, the unlikely EC mechanism is based on

**Table 3. Kinetic Parameters for the E Mechanism at DCE/Water Interfaces**

ion/ionophore	$k^0/\text{cm s}^{-1}$	$\alpha$	$D_c/\text{cm}^2 \text{s}^{-1}$	$k_{\text{DCE}}^0/k_{\text{PVC}}^0$	$D_{c,\text{DCE}}/D_{c,\text{PVC}}$
$\text{Ag}^+/1$	$2.6 \times 10^{-2}$	0.48	$3.0 \times 10^{-6}$	4.2	63
$\text{K}^+/2$	$1.1 \times 10^{-2}$	0.33	$1.1 \times 10^{-6}$	1.3	11
$\text{Ba}^{2+}/3^a$	$1.2 \times 10^{-2}$	0.45	$3.7 \times 10^{-6}$	1.2	52
$\text{Ca}^{2+}/3$	$7.1 \times 10^{-4}$	0.39	—	0.19	—
$\text{Pb}^{2+}/4$	$4.4 \times 10^{-4}$	$0.50^b$	—	0.45	—

<sup>a</sup> From ref 8a. <sup>b</sup>  $z = 0.85$ .

the transfer of intermediate 1:2 or 1:1 ion–ionophore complexes as the E process and is followed by their complexation with additional ionophore molecule(s) in the bulk membrane as the C process. The following complexation process is highly favored thermodynamically so that the transfer of the intermediate complexes and the dissociation of the overall complexes must be unrealistically fast to be consistent with the quasi-reversible CVs.

**Facilitated IT at DCE/Water Microinterfaces.** We employed micropipet voltammetry to determine rates for the IT processes facilitated by ionophores 1–4 at DCE/water interfaces, which turned out to be similar to those at plasticized PVC membrane/water interfaces. With a DCE-filled micropipet (cell 2), the forward potential sweep drives the transfer of an ion from the outer aqueous phase into the inner DCE phase. The resulting sigmoidal wave (Figures 4 and 5) confirms the nonlinear diffusion of the transferring aqueous ion to the microinterface. For sufficiently fast transfers of  $\text{Ag}^+$  (Figure 4),  $\text{K}^+$  (Figure 5a), and  $\text{Ba}^{2+}$  (Figure 8 in ref 8a), the reverse potential sweep gives a peak-shaped wave because the inner pipet wall hinders the diffusion of ion–ionophore complexes in the DCE solution. In fact, the transient reverse response varies with  $\nu$  as clearly seen for quasi-reversible  $\text{Ag}^+$  and  $\text{Ba}^{2+}$  transfers. In contrast, the reverse peak of slower  $\text{Pb}^{2+}$  transfer is small and widely separated from the forward wave to overlap with the potential window limit at  $E - E^0 > -0.05$  V, where the background-subtracted response is distorted (Figure 5c). No reverse peak was observed for electrochemically irreversible  $\text{Ca}^{2+}$  transfer (Figure 5b).

Quasi-reversible CVs of facilitated  $\text{Ag}^+$ ,  $\text{K}^+$ , and  $\text{Ba}^{2+}$  transfers at DCE/water microinterfaces fit well with theoretical voltammograms based on the E mechanism to give all kinetic and thermodynamic parameters in the Butler–Volmer-type model as well as  $D_w$  and  $D_c$  values (Table 3).<sup>8a</sup> Irreversible CVs of facilitated  $\text{Ca}^{2+}$  and  $\text{Pb}^{2+}$  transfers were also numerically analyzed using the E mechanism with  $E^0$  values determined by potentiometry (see Supporting Information) to yield  $k^0$  and  $\alpha$  values (Table 3). The theoretical micropipet CVs of quasi-reversible and irreversible IT were simulated as reported elsewhere.<sup>8a</sup> Overall, the  $k^0$  values thus obtained at DCE/water microinterfaces are nearly as low as those at PVC membrane/water interfaces. Facilitated  $\text{Ag}^+$  and  $\text{Ba}^{2+}$  transfers at DCE/water microinterfaces give  $\alpha$  values of  $\sim 0.5$  to confirm the one-step E mechanism. Smaller  $\alpha$  values of 0.33 and 0.39 for  $\text{K}^+$  and  $\text{Ca}^{2+}$  transfers, respectively, are ascribed to a double layer effect. A more significant double layer effect is apparent in the voltammogram of facilitated  $\text{Pb}^{2+}$  transfer, which is broader than expected for  $z = 2$  and  $\alpha = 0.5$  to give an effective  $z$  value of 0.85 for a normal  $\alpha$  value of 0.5.

The EC mechanism is excluded also for facilitated IT at DCE/water microinterfaces. For any of the facilitated IT reactions examined in this work,  $k^0$  values with DCE and *o*NPOE/PVC

**Table 4. Thermodynamic and Kinetic Parameters for the EC Mechanism at DCE/Water Interfaces**

ion/ionophore	$\beta_n (n)$	$E^0 - E_i^0/V^a$	$k_i^0/\text{cm s}^{-1}$	$\alpha_i$	$k_s/M^{-1} \text{s}^{-1}$
$\text{Ag}^+/1$	$2.5 \times 10^{12} (1)^b$	0.63	$4.5 \times 10^3$	0.50	$>1.7 \times 10^{18}$
$\text{K}^+/2$	$6.3 \times 10^{14} (1)^c$	0.77	$2.4 \times 10^2$	0.33	$>2.9 \times 10^{21}$

<sup>a</sup> Calculated using eq 5. <sup>b</sup> From ref 36. <sup>c</sup> From ref.37.

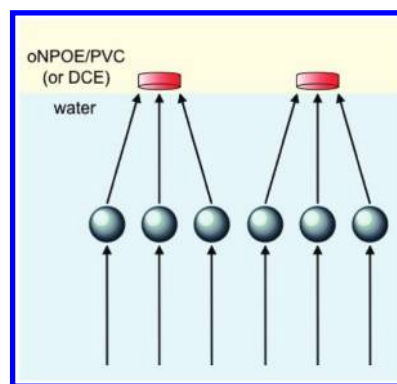


**Figure 6.** Scheme of the nonlinear diffusion of aqueous ions to membraneous ionophore molecules for their collision and subsequent complexation at the interface.

systems are relatively similar to each other (see  $k_{\text{DCE}}^0/k_{\text{PVC}}^0$  in Table 3) in contrast to very different  $D_c$  values in these media (see  $D_{c,\text{DCE}}/D_{c,\text{PVC}}$ , which correspond to much higher viscosity of the *o*NPOE/PVC membrane than the DCE phase (13.8 and 0.779 mPa s for pure *o*NPOE and DCE, respectively<sup>26</sup>). This little viscosity effect on IT kinetics is inconsistent with the EC mechanism, where simple IT is slower with a more viscous media<sup>21</sup> (e.g.,  $k_i^0 = 6$  cm/s with DCE<sup>34</sup> and 0.01 cm/s with *o*NPOE-plasticized PVC membrane<sup>35</sup> for tetraethylammonium transfer). In addition, the numerical analysis of quasi-reversible CVs of  $\text{K}^+$  and  $\text{Ag}^+$  transfers at DCE/water microinterfaces using the EC mechanism (Figures S-6 and S-7, respectively; see Supporting Information) shows that simple IT and the association of ion–ionophore complexes must be unrealistically fast (Table 4) to satisfy the apparently  $E_qC_r$  scheme. These requirements are due to strong interactions of these ions with the corresponding ionophores in the DCE phase ( $\beta_1 = 2.5 \times 10^{12}$  and  $6.3 \times 10^{14}$  for  $\text{Ag}^+$ <sup>36</sup> and  $\text{K}^+$ ,<sup>37</sup> respectively) and are also expected for strongly facilitated transfers of  $\text{Ba}^{2+}$ ,  $\text{Ca}^{2+}$ , and  $\text{Pb}^{2+}$ , thereby excluding the EC mechanism.

**Molecular Level Models for the E Mechanism.** We further analyzed the  $k^0$  values for the E mechanism at the molecular level to find that the rate-determining step of bimolecular (or multi-molecular) IT as facilitated by ionophores is their ion recognition at the very interface rather than the nonlinear diffusion of an aqueous ion for its collision with the excess amount of ionophore at the interface (Figure 6). Specifically, a rate constant for the diffusion-limited collision,  $k$ , was estimated using the effective medium theory<sup>24,38</sup> to yield

$$k = 4D_w r l N_A L_T \quad (7)$$

where  $r$  is the radius of the disk-like adsorber that represents an ionophore, and  $l$  is the depth of the interfacial region where the ionophore is available for collision with aqueous ions. The  $k^0$  values at either PVC/water or DCE/water interfaces are more

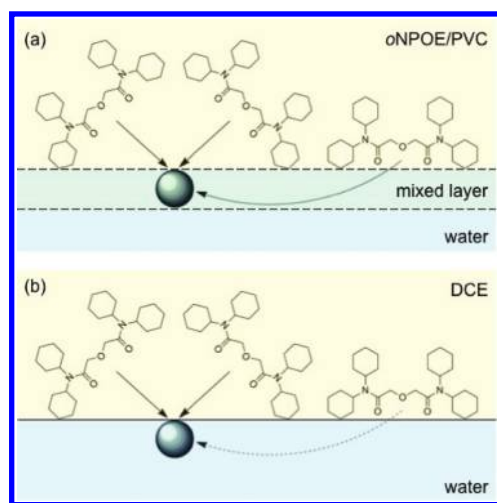


**Figure 7.** Scheme of the formation of 1:3  $\text{Ca}^{2+}$ –ionophore 3 complexes at (a) a *o*NPOE-plasticized PVC membrane/water interface with a thicker mixed layer and (b) a sharper DCE/water interface.

than 3 orders of magnitude lower than  $k$  values of 30–90 cm/s in eq 7 with  $D_w = 1.5 \times 10^{-5}$  cm<sup>2</sup>/s,  $r = 1.5$  nm,  $l = 3$  nm, and  $L_T = 0.02$ – $0.06$  M. Similar  $k$  values were also estimated for bimolecular ET reactions at the ITIES.<sup>39</sup>

The unique feature of the E mechanism at the molecular level is the formation of three-dimensional ion–ionophore complexes at the two-dimensional interface, which contrasts to homogeneous ion–ionophore complexation in the EC mechanism. We speculate that this feature explains why  $\text{Ca}^{2+}$  transfer is more rapid at PVC membrane/water interfaces than at DCE/water interfaces ( $k_{\text{DCE}}^0/k_{\text{PVC}}^0 = 0.19$ ) while the  $\text{Ba}^{2+}$  transfer facilitated by the same ionophore is similarly fast at these interfaces ( $k_{\text{DCE}}^0/k_{\text{PVC}}^0 = 1.2$ ). Geometrically, a calcium ion is readily accessible to two molecules of ionophore 3 from the nonaqueous side of the interface, while the third ionophore molecule must bind to the ion from its aqueous side to form three-dimensional 1:3 complexes<sup>40</sup> at the interface, which is required for the E mechanism as discussed above. Importantly, polar *o*NPOE molecules are dominant at the surface of an *o*NPOE-plasticized polymer membrane in contact with water<sup>41</sup> to form a mixed layer,<sup>42</sup> thereby allowing a lipophilic ionophore molecule to more easily access to the ion from its aqueous side through the mixed layer (Figure 7a). In contrast, less polar DCE forms a sharper interface with a thinner mixed layer, which slows down the access of the third ionophore molecule to the ion (Figure 7b). The solvent-dependent accessibility of ionophore to an ion from its aqueous side is less important for the formation of 1:2  $\text{Ba}^{2+}$ –ionophore 3 complexes<sup>33</sup> to yield similar  $k^0$  values at both interfaces. Kinetically, the E mechanism is not simply the extreme case of the EC mechanism where ion–ionophore complexation occurs similarly both in the bulk solution and at the interface.

## CONCLUSION

In this work, we revealed the electrochemical kinetics of facilitated IT at polymer membrane/water interfaces to resolve long-standing controversies on the intrinsic rate and mechanism of this charge transfer process with practical importance and fundamental uniqueness. The kinetics observed with highly selective ionophores 1–4 is slow enough to fully assess E and EC mechanisms, which supports the former mechanism and

excludes the latter. Our data also suggests that, at the molecular level, the E mechanism is controlled by three-dimensional ion–ionophore complexation at the two-dimensional interface to serve as a unique molecular-recognition system. In contrast, the three-dimensional accessibility of an ion is guaranteed for homogeneous complexation in the EC mechanism. Moreover, the theoretical assessment of the EC mechanism using kinetic voltammograms confirms that this mechanism is generally invalid when ionophore-mediated IT is both thermodynamically and kinetically facile. In fact, this is the case for most of the facilitated IT reactions reported so far, thereby augmenting the significance of this work.

The power of our double-polymer-modified electrodes for the quantitative study of IT kinetics was demonstrated in this work to make important findings for voltammetric/amperometric ion sensing by these electrodes. Interestingly, we found that the  $\text{Ca}^{2+}$  transfer facilitated by ionophore 3 is faster at PVC membrane/water interfaces than at DCE/water interfaces. This accelerating effect from a viscous medium is significant because faster transfer of a target ion is required for higher sensitivity and selectivity while a viscous nonaqueous medium is the essential component of a robust sensing device.<sup>43</sup> Moreover, the comparison of facilitated  $\text{Ca}^{2+}$  and  $\text{Ba}^{2+}$  transfers demonstrates not only the feasibility of the voltammetric detection of multiple ions using a single electrode<sup>18c</sup> but also the dual ion selectivity of the voltammetric/amperometric approach as controlled both thermodynamically and kinetically. In contrast, ionophore-based potentiometric and optical sensors detect only one target ion with the highest thermodynamic selectivity as assumed in the phase boundary potential model,<sup>1b</sup> although this study indicates that facilitated IT may not be rapid enough to always behave as a Nernstian process.<sup>11c</sup> Finally, voltammetric and amperometric applications of the extremely selective ionophores that were developed for the potentiometric and optical sensors are highly attractive as more advanced sensing technologies.

## ASSOCIATED CONTENT

**Supporting Information.** CV characterization of PVC/PEDOT- $\text{C}_{14}$ -modified electrodes, voltammetric determination of diffusion coefficients of ion–ionophore complexes in plasticized PVC membranes, model for the EC mechanism and its use for the numerical analysis of CVs, and potentiometric determination of formal potentials for the analysis of irreversible micro-pipet CVs. This material is available free of charge via the Internet at <http://pubs.acs.org>.

## AUTHOR INFORMATION

### Corresponding Author

amemiya@pitt.edu

### Present Addresses

<sup>†</sup>Department of Applied Chemistry, Graduate School of Engineering, Kyushu University, Nishi-Ku, Fukuoka 819-0395, Japan.

## ACKNOWLEDGMENT

This work was supported by a CAREER award from the National Science Foundation (CHE-0645623). We thank Prof. Toshiyuki Osakai, Department of Chemistry, Graduate School of Science, Kobe University, for valuable discussion.

## REFERENCES

- (1) (a) Meyerhoff, M. E.; Opdycke, W. N. *Adv. Clin. Chem.* **1986**, 25, 1. (b) Bakker, E.; Bühlmann, P.; Pretsch, E. *Chem. Rev.* **1997**, 97, 3083. (c) Buck, R. P.; Lindner, E. *Acc. Chem. Res.* **1998**, 31, 257. (d) Buck, S. M.; Koo, Y. E. L.; Park, E.; Xu, H.; Philbert, M. A.; Brasuel, M. A.; Kopelman, R. *Curr. Opin. Chem. Biol.* **2004**, 8, 540. (e) Bakker, E.; Pretsch, E. *Angew. Chem., Int. Ed.* **2007**, 46, 5660. (f) Amemiya, S. In *Handbook of Electrochemistry*; Zoski, C. G., Ed.; Elsevier: New York, 2007; p 261.
- (2) Nghiem, L. D.; Mornane, P.; Potter, I. D.; Perera, J. M.; Cattrall, R. W.; Kolev, S. D. *J. Membr. Sci.* **2006**, 281, 7.
- (3) (a) Bühlmann, P.; Pretsch, E.; Bakker, E. *Chem. Rev.* **1998**, 98, 1593. (b) Umezawa, Y.; Bühlmann, P.; Umezawa, K.; Tohda, K.; Amemiya, S. *Pure Appl. Chem.* **2000**, 72, 1851. (c) Umezawa, Y.; Umezawa, K.; Bühlmann, P.; Hamada, N.; Aoki, H.; Nakanishi, J.; Sato, M.; Xiao, K. P.; Nishimura, Y. *Pure Appl. Chem.* **2002**, 74, 923. (d) Umezawa, Y.; Bühlmann, P.; Umezawa, K.; Hamada, N. *Pure Appl. Chem.* **2002**, 74, 995.
- (4) (a) Qin, Y.; Mi, Y.; Bakker, E. *Anal. Chim. Acta* **2000**, 421, 207. (b) Szigeti, Z.; Malon, A.; Vigassy, T.; Csokai, V.; Grun, A.; Wygladacz, K.; Ye, N.; Xu, C.; Chebny, V. J.; Bitter, I.; Rathore, R.; Bakker, E.; Pretsch, E. *Anal. Chim. Acta* **2006**, 572, 1.
- (5) (a) Vanysek, P.; Ramirez, L. B. *J. Chil. Chem. Soc.* **2008**, 53, 1455. (b) Girault, H. H. In *Electroanalytical Chemistry*; Bard, A. J., Zoski, C. G., Eds.; Taylor & Francis: Boca Raton, FL, 2010; Vol. 23, p 1. (c) Liu, S. J.; Li, Q.; Shao, Y. H. *Chem. Soc. Rev.* **2011**, 40, 2236.
- (6) Kakutani, T.; Nishiwaki, Y.; Osakai, T.; Senda, M. *Bull. Chem. Soc. Jpn.* **1986**, 59, 781.
- (7) E and EC mechanisms are also known as “transfer by interfacial complexation(TIC)” and “ion transfer followed by complexation in the organic phase(TOC),” respectively; see: Shao, Y.; Osborne, M. D.; Girault, H. H. *J. Electroanal. Chem.* **1991**, 318, 101.
- (8) (a) Rodgers, P. J.; Amemiya, S. *Anal. Chem.* **2007**, 79, 9276. (b) Cui, R.; Li, Q.; Gross, D. E.; Meng, X.; Li, B.; Marquez, M.; Yang, R.; Sessler, J. L.; Shao, Y. *J. Am. Chem. Soc.* **2008**, 130, 14364.
- (9) (a) Shao, Y.; Mirkin, M. V. *J. Am. Chem. Soc.* **1997**, 119, 8103. (b) Yuan, Y.; Shao, Y. H. *J. Phys. Chem. B* **2002**, 106, 7809. (c) Cai, C. X.; Tong, Y. H.; Mirkin, M. V. *J. Phys. Chem. B* **2004**, 108, 17872.
- (10) Samec, Z.; Homolka, D.; Marecek, V. *J. Electroanal. Chem.* **1982**, 135, 265.
- (11) (a) Buck, R. P. In *Ion-Transfer Kinetics: Principles and Applications*; Sandifer, J. R., Ed.; VCH: New York, 1995; p 19. (b) Sandifer, J. R.; Iglehart, M. L.; Buck, R. P. *Anal. Chem.* **1989**, 61, 1624. (c) Buck, R. P. *Anal. Chem.* **1968**, 40, 1439.
- (12) Senda, M. *J. Electroanal. Chem.* **1994**, 378, 215.
- (13) (a) Bakker, E.; Willer, M.; Pretsch, E. *Anal. Chim. Acta* **1993**, 282, 265. (b) Sokalski, T.; Ceresa, A.; Zwickl, T.; Pretsch, E. *J. Am. Chem. Soc.* **1997**, 119, 11347.
- (14) Bakker, E.; Pretsch, E.; Bühlmann, P. *Anal. Chem.* **2000**, 72, 1127.
- (15) Kolev, S. D.; Argiropoulos, G.; Cattrall, R. W.; Hamilton, I. C.; Paimin, R. *J. Membr. Sci.* **1997**, 137, 261.
- (16) (a) Lee, H. J.; Beattie, P. D.; Seddon, B. J.; Osborne, M. D.; Girault, H. H. *J. Electroanal. Chem.* **1997**, 440, 73. (b) Lee, H. J.; Beriet, C.; Girault, H. H. *J. Electroanal. Chem.* **1998**, 453, 211.
- (17) Armstrong, R. D. *J. Electroanal. Chem.* **1988**, 245, 113.
- (18) (a) Guo, J.; Amemiya, S. *Anal. Chem.* **2006**, 78, 6893. (b) Kim, Y.; Amemiya, S. *Anal. Chem.* **2008**, 80, 6056. (c) Kim, Y.; Rodgers, P. J.; Ishimatsu, R.; Amemiya, S. *Anal. Chem.* **2009**, 81, 7262.
- (19) (a) Si, P. C.; Bakker, E. *Chem. Commun.* **2009**, 5260. (b) Yoshida, Y.; Yamaguchi, S.; Maeda, K. *Anal. Sci.* **2010**, 26, 137.
- (20) Zhang, J.; Harris, A. R.; Cattrall, R. W.; Bond, A. M. *Anal. Chem.* **2010**, 82, 1624.
- (21) (a) Kakiuchi, T. *J. Electroanal. Chem.* **1992**, 322, 55. (b) Samec, Z.; Langmaier, J.; Trojanek, A. *J. Electroanal. Chem.* **1997**, 426, 37. (c) Marcus, R. A. *J. Chem. Phys.* **2000**, 113, 1618.
- (22) Breiby, D. W.; Samuelsen, E. J.; Groenendaal, L.; Struth, B. *J. Polym. Sci., Part B: Polym. Phys.* **2003**, 41, 945.
- (23) Amemiya, S.; Yang, X.; Wazenegger, T. L. *J. Am. Chem. Soc.* **2003**, 125, 11832.
- (24) Ishimatsu, R.; Kim, J.; Jing, P.; Striemer, C. C.; Fang, D. Z.; Fauchet, P. M.; McGrath, J. L.; Amemiya, S. *Anal. Chem.* **2010**, 82, 7127.
- (25) Bard, A. J.; Faulkner, L. R. *Electrochemical Methods: Fundamentals and Applications*; 2nd ed.; John Wiley & Sons: New York, 2001; p243.
- (26) Samec, Z. *Pure Appl. Chem.* **2004**, 76, 2147.
- (27) (a) Bodor, S.; Zook, J. M.; Lindner, E.; Toth, K.; Gyurcsanyi, R. E. *Analyst* **2008**, 133, 635. (b) Bodor, S.; Zook, J. M.; Lindner, E.; Toth, K.; Gyurcsanyi, R. E. *J. Solid State Electrochem.* **2009**, 13, 171.
- (28) (a) Yuan, Y.; Amemiya, S. *Anal. Chem.* **2004**, 76, 6877. (b) Yuan, Y.; Wang, L.; Amemiya, S. *Anal. Chem.* **2004**, 76, 5570.
- (29) Ceresa, A.; Bakker, E.; Hattendorf, B.; Günther, D.; Pretsch, E. *Anal. Chem.* **2001**, 73, 343.
- (30) Bard, A. J.; Faulkner, L. R. *Electrochemical Methods: Fundamentals and Applications*; 2nd ed.; John Wiley & Sons: New York, 2001; p 499.
- (31) Langmaier, J.; Stejskalova, K.; Samec, Z. *J. Electroanal. Chem.* **2002**, 521, 81.
- (32) Houston, P. L. *Chemical Kinetics and Reactions Dynamics*; Dover Publications, Inc.: New York, 2001.
- (33) Wang, E.; Yu, Z.; Xu, C.; Qi, D. *Anal. Sci.* **1993**, 9, 405.
- (34) Wang, Y.; Velmurugan, J.; Mirkin, M. V.; Rodgers, P. J.; Kim, J.; Amemiya, S. *Anal. Chem.* **2010**, 82, 77.
- (35) Langmaier, J.; Stejskalova, K.; Samec, Z. *J. Electroanal. Chem.* **2002**, 521, 81.
- (36) Dwyer, P.; Cunnane, V. J. *J. Electroanal. Chem.* **2005**, 581, 16.
- (37) Osborne, M. D.; Girault, H. H. *Electroanalysis* **1995**, 7, 425.
- (38) (a) Berg, H. C. *Random Walks in Biology*; Princeton University Press: Princeton, NJ, 1993; p 17. (b) Kim, E.; Xiong, H.; Striemer, C. C.; Fang, D. Z.; Fauchet, P. M.; McGrath, J. L.; Amemiya, S. *J. Am. Chem. Soc.* **2008**, 130, 4230 and references cited therein.
- (39) (a) Osakai, T.; Hotta, H.; Sugihara, T.; Nakatani, K. *J. Electroanal. Chem.* **2004**, 571, 201. (b) Osakai, T.; Okamoto, M.; Sugihara, T.; Nakatani, K. *J. Electroanal. Chem.* **2009**, 628, 27.
- (40) (a) Neupert-Laves, K.; Dobler, M. *J. Crystallogr. Spectrosc. Res.* **1982**, 12, 287. (b) Schefer, U.; Ammann, D.; Pretsch, E.; Oesch, U.; Simon, W. *Anal. Chem.* **1986**, 58, 2282.
- (41) Clarke, M. L.; Wang, J.; Chen, Z. *Anal. Chem.* **2003**, 75, 3275.
- (42) Jorge, M.; Natalia, M.; Cordeiro, D. S. *J. Phys. Chem. B* **2008**, 112, 2415.
- (43) Amemiya, S.; Kim, Y.; Ishimatsu, R.; Kabagambe, B. *Anal. Bioanal. Chem.* **2011**, 399, 571.